# Anisotropic diffusion cannot explain TeV halo observations

**Pedro de la Torre Luque**     OKC, Stockholm University

pedro.delatorreluque@fysik.su.se

# TeV halos – a few observations

Unexpected emission at high energies around PWNe :
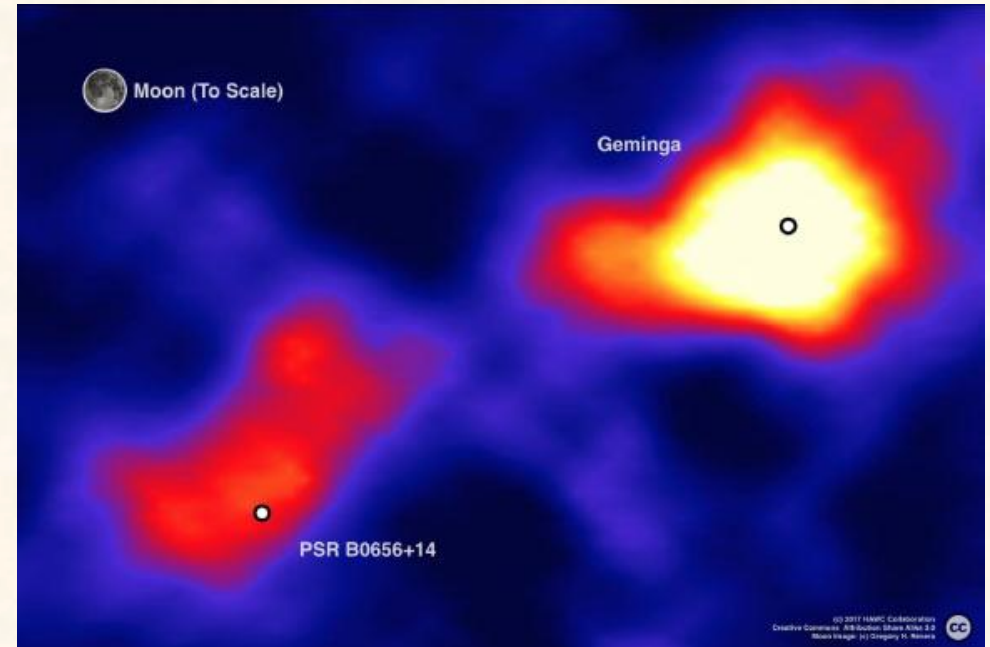
    - PWN ~ 0.1 pc - few pc
    - TeV halo Geminga 25 pc (2°)

Gamma-ray spectrum well compatible with **IC emission**

Emission profile ~1/r (**diffusive profile**)
Nevertheless, much less extended than expected
assuming the typical **Diff. Coeff**. (**100 times smaller**)

A few TeV halos have been found - **all of them seem to be symmetric and explained by a similar Diff. Coeff.**



Abysekara et al. 2017

2

# TeV halos – a few observations

Unexpected emission at high energies around PWNe :
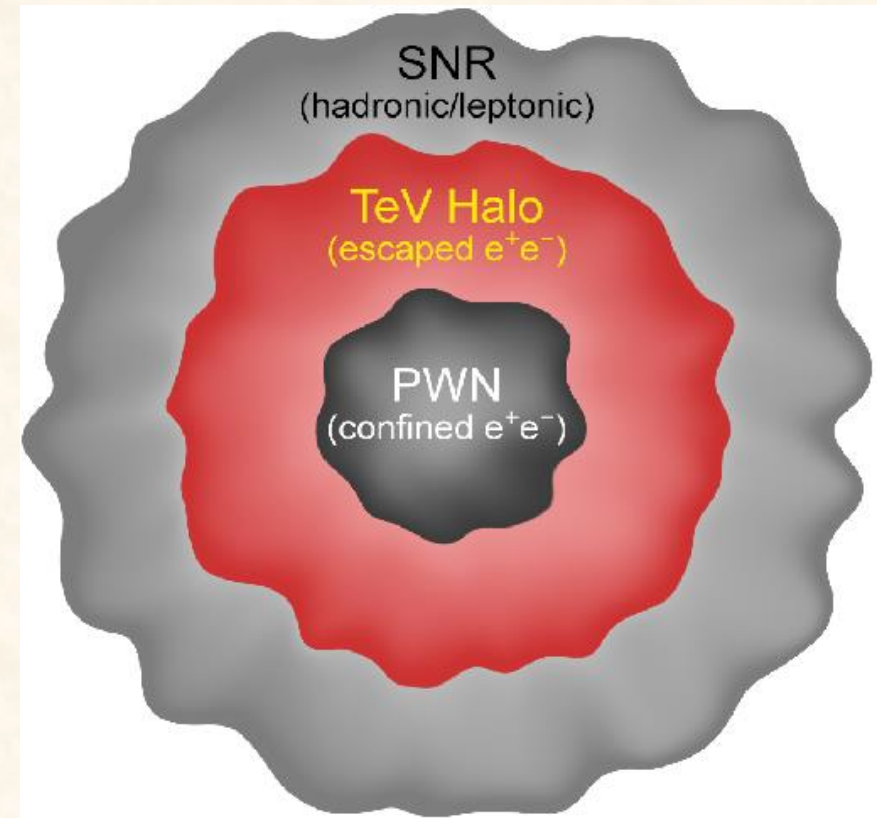
    - PWN ~ 0.1 pc - few pc
    - TeV halo Geminga 25 pc (2°)

Gamma-ray spectrum well compatible with **IC emission**

Emission profile ~1/r (**diffusive profile**)
Nevertheless, much less extended than expected
assuming the typical **Diff. Coeff**. (**100 times smaller**)

A few TeV halos have been found - **all of them seem to be symmetric and explained by a similar Diff. Coeff.**

# TeV halos – a few observations

Different theories try to explain the origin of these halos

o Ballistic propagation (Recchia et al. PRD 104, 123017, 2021)
o Self-generation of turbulence (Evoli et al. PRD 98, 063017, 2018)
o Anisotropic diffusion (Ruo-Yu Liu et al. PRL 123, 221103, 2019)
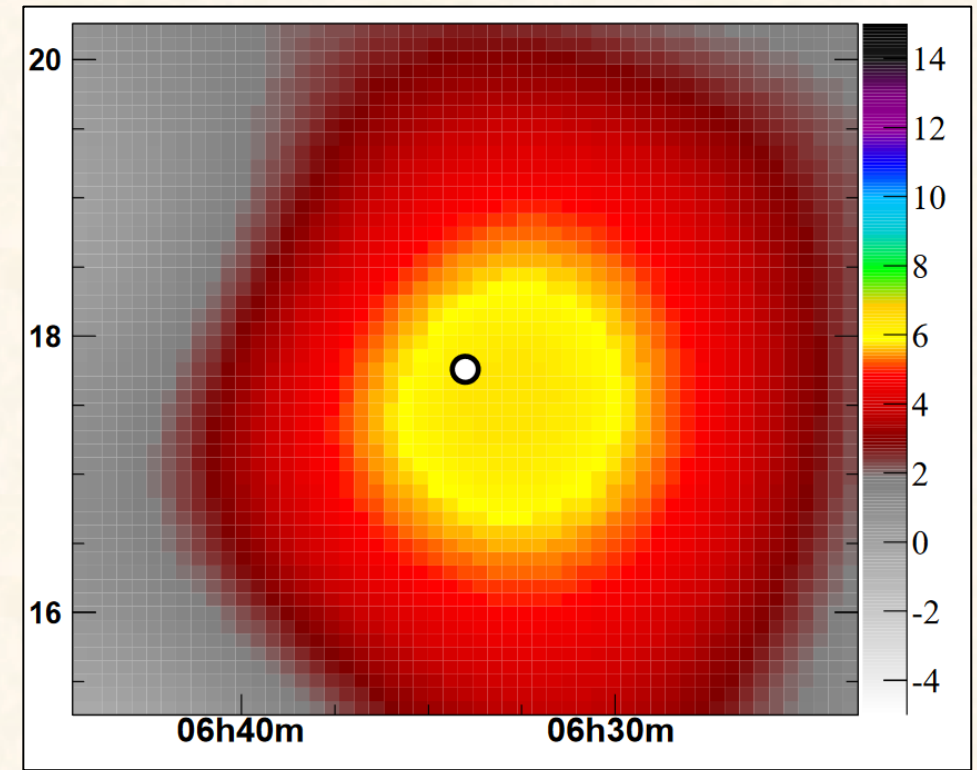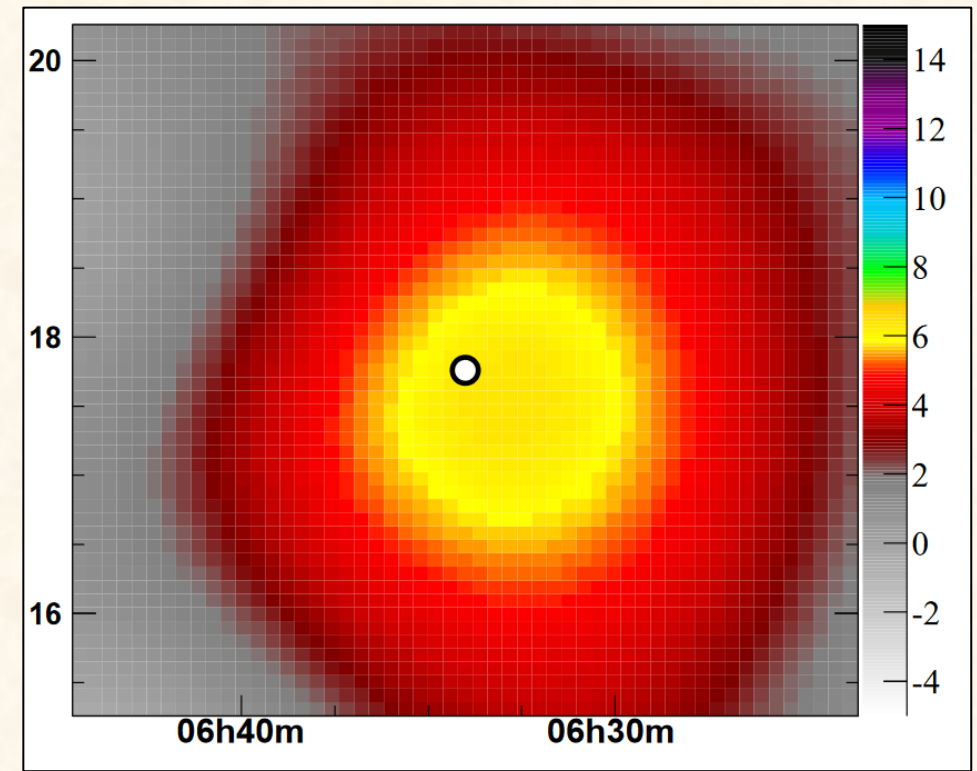
Abysekara et al. 2017

# TeV halos – a few observations

Different theories try to explain the origin of these halos

- Ballistic propagation (Recchia et al. PRD 104, 123017, 2021)
- Self-generation of turbulence (Evoli et al. PRD 98, 063017, 2018)
- Anisotropic diffusion (Ruo-Yu Liu et al. PRL 123, 221103, 2019)

If turbulence is inhibited in the direction perpendicular to the magnetic field around the PWN and the magnetic field direction is aligned with our line of sight we can reproduce Geminga observations!

Abysekara et al. 2017
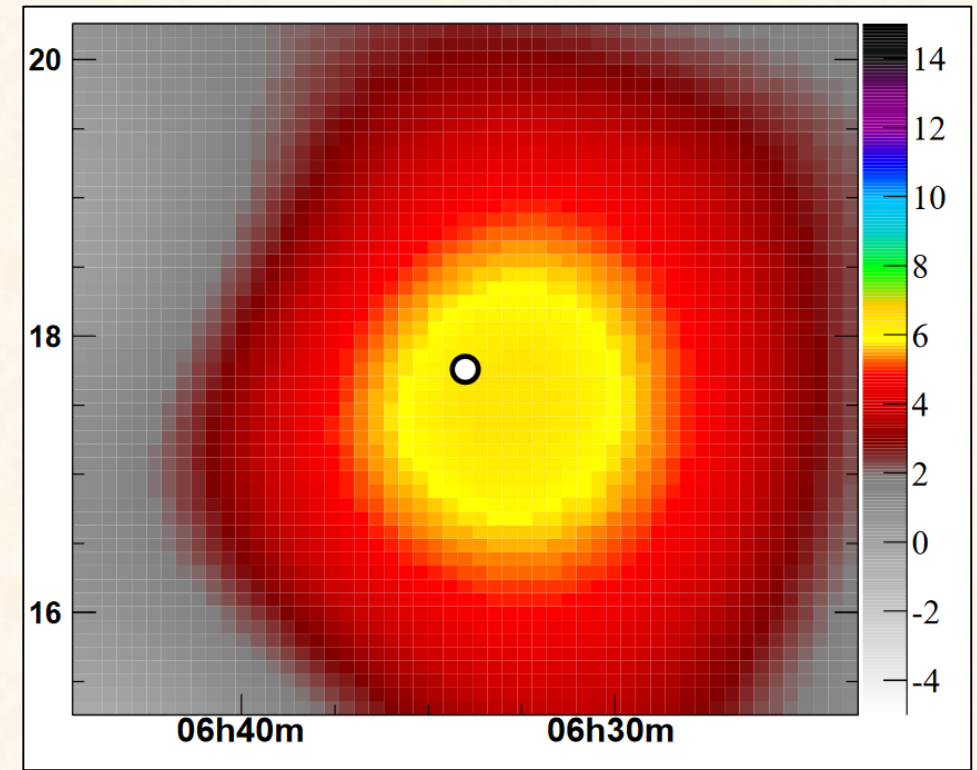
# TeV halos – a few observations

Different theories try to explain the origin of these halos

o Ballistic propagation (Recchia et al. PRD 104, 123017, 2021)
o Self-generation of turbulence (Evoli et al. PRD 98, 063017, 2018)
o Anisotropic diffusion (Ruo-Yu Liu et al. PRL 123, 221103, 2019) **?**

If turbulence is inhibited in the direction perpendicular to the magnetic field around the PWN and the magnetic field direction is aligned with our line of sight we can reproduce Geminga observations!
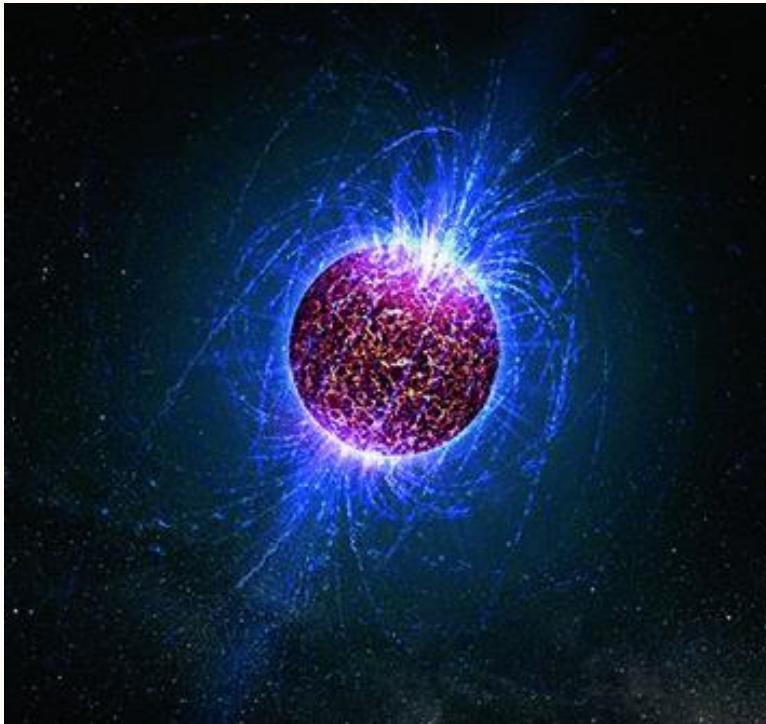
A few TeV halos have been found - **all of them seem to be nearly symmetric**

Abysekara et al. 2017

# Anisotropic diffusion

$$\frac{\partial u}{\partial t}(r,z,t,E_e) = \frac{1}{r}\frac{\partial}{\partial r}\left(rD_r\frac{\partial u}{\partial r}(r,z,t,E_e)\right) + \frac{\partial}{\partial z}\left(D_z\frac{\partial u}{\partial z}(r,z,t,E_e)\right) +$$
$$+ \mathcal{S}(r,z,t,E_e) + \frac{\partial}{\partial E_e}\left(\frac{\partial E_e}{\partial t}u(r,z,t,E_e)\right)$$

In the vicinity of the source, the **magnetic field** resembles a dipole, so that the magnetic lines follow the direction of the poles (**z axis**).

Propagation of particles along the lines (parallel to the **B** direction) is faster than in the **perpendicular direction** (**r axis**), creating a cylindrically symmetric diffusion around the PWN (around the z axis)
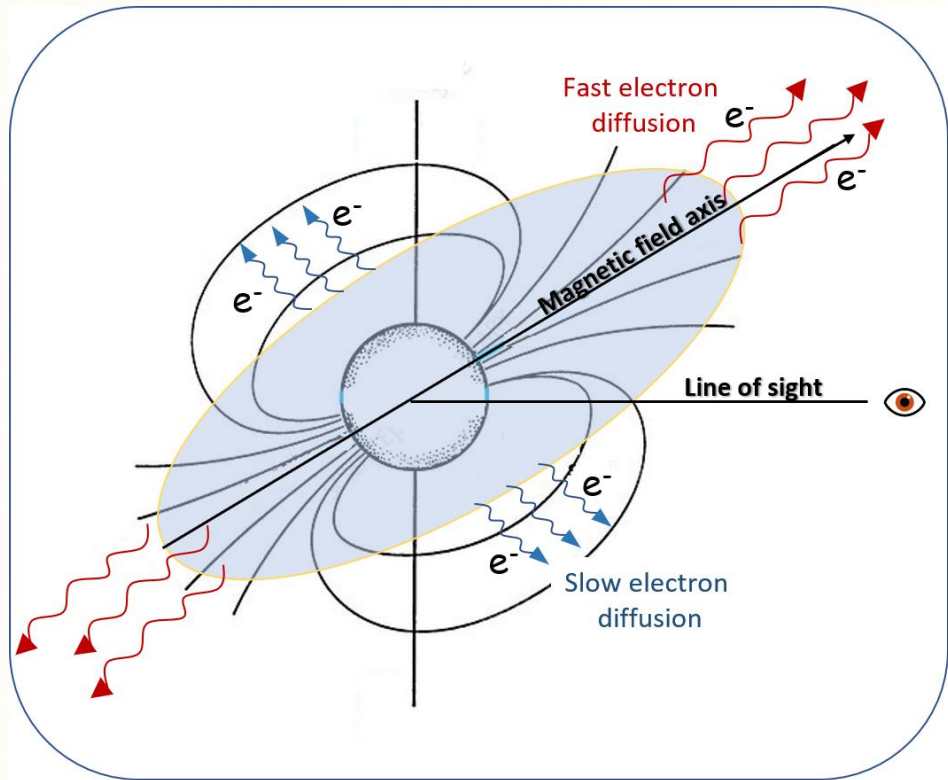
Yan et al. ApJ, 673:942-953, 2008

$$\boldsymbol{D_r = X\,D_z} \;\; ; \;\; X = M_A^4$$

$M_A \rightarrow$ Alfvenic Mach number

$$M_A \sim \left.\frac{\delta B}{B_0}\right|_{L_{Inj}}$$

# Anisotropic diffusion

$$\frac{\partial u}{\partial t}(r, z, t, E_e) = \frac{1}{r}\frac{\partial}{\partial r}\left(rD_r\frac{\partial u}{\partial r}(r, z, t, E_e)\right) + \frac{\partial}{\partial z}\left(D_z\frac{\partial u}{\partial z}(r, z, t, E_e)\right) +$$

$$+\mathcal{S}(r, z, t, E_e) + \frac{\partial}{\partial E_e}\left(\frac{\partial E_e}{\partial t}u(r, z, t, E_e)\right)$$



In the vicinity of the source, the **magnetic field** resembles a dipole, so that the magnetic lines follow the direction of the poles (**z axis**).

Propagation of particles along the lines (parallel to the **B** direction) is faster than in the **perpendicular direction** (**r axis**), creating a cylindrically symmetric diffusion around the PWN (around the z axis)
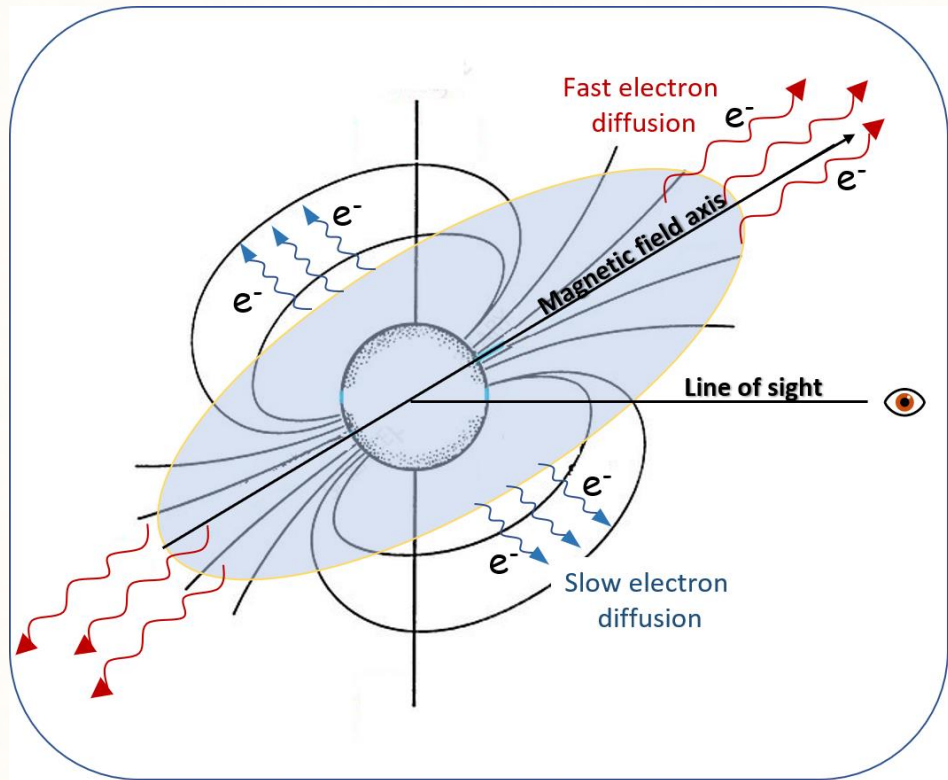
Yan et al. ApJ, 673:942-953, 2008

$$\boldsymbol{D_r = X\,D_z}\;;\;X = M_A^4$$

$M_A \rightarrow$ Alfvenic Mach number

$$M_A \sim \left.\frac{\delta B}{B_0}\right|_{L_{Inj}}$$

We define the inclination angle, $\psi_{Incl}$, as the angle between the magnetic field axis and the line of sight of the observer.

8

# Anisotropic diffusion

$$\frac{\partial u}{\partial t}(r,z,t,E_e) = \frac{1}{r}\frac{\partial}{\partial r}\left(rD_r\frac{\partial u}{\partial r}(r,z,t,E_e)\right) + \frac{\partial}{\partial z}\left(D_z\frac{\partial u}{\partial z}(r,z,t,E_e)\right) +$$

$$+ \mathcal{S}(r,z,t,E_e) + \frac{\partial}{\partial E_e}\left(\frac{\partial E_e}{\partial t}u(r,z,t,E_e)\right)$$



We define the inclination angle, $\psi_{Incl}$, as the angle between the magnetic field axis and the line of sight of the observer.

In the vicinity of the source, the **magnetic field** resembles a dipole, so that the magnetic lines follow the direction of the poles (**z axis**).

Propagation of particles along the lines (parallel to the **B** direction) is faster than in the **perpendicular direction** (**r axis**), creating a cylindrically symmetric diffusion around the PWN (around the z axis)

Yan et al. ApJ, 673:942-953, 2008

$$D_r = X\,D_z \;\; ; \;\; X = M_A^4$$
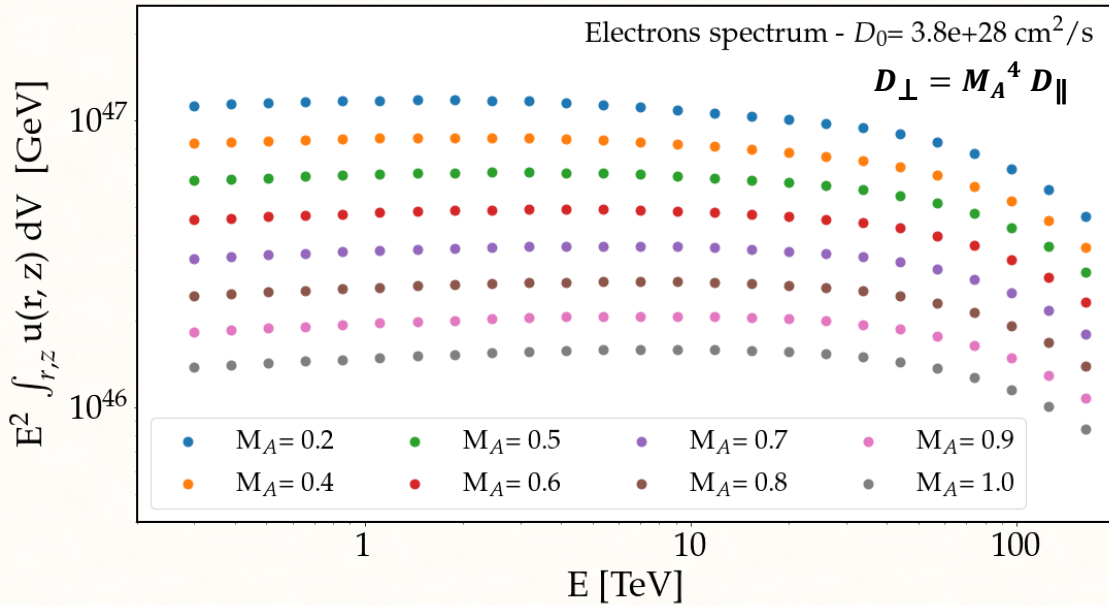
$M_A \rightarrow$ Alfvenic Mach number

$$M_A \sim \frac{\delta B}{B_0}\bigg|_{L_{Inj}}$$

Can it explain TeV halos for normal values of the diffusion coefficient?

9

# Anisotropic diffusion

$$\frac{\partial u}{\partial t}(r, z, t, E_e) = \frac{1}{r}\frac{\partial}{\partial r}\left(r D_r \frac{\partial u}{\partial r}(r, z, t, E_e)\right) + \frac{\partial}{\partial z}\left(D_z \frac{\partial u}{\partial z}(r, z, t, E_e)\right) +$$

$$+ \mathcal{S}(r, z, t, E_e) + \frac{\partial}{\partial E_e}\left(\frac{\partial E_e}{\partial t} u(r, z, t, E_e)\right)$$

### 5.5° window around the PWN



Leptons are injected with a source term following:

$$\mathcal{S}(r, z, t, E_e) = \mathcal{S}_0 (1 + t/\tau_0)^{-\frac{n+1}{n-1}}\left(E_e/\text{GeV}\right)^{-\alpha} e^{-E_e/E_{\text{cut}}} \delta(r, z)$$
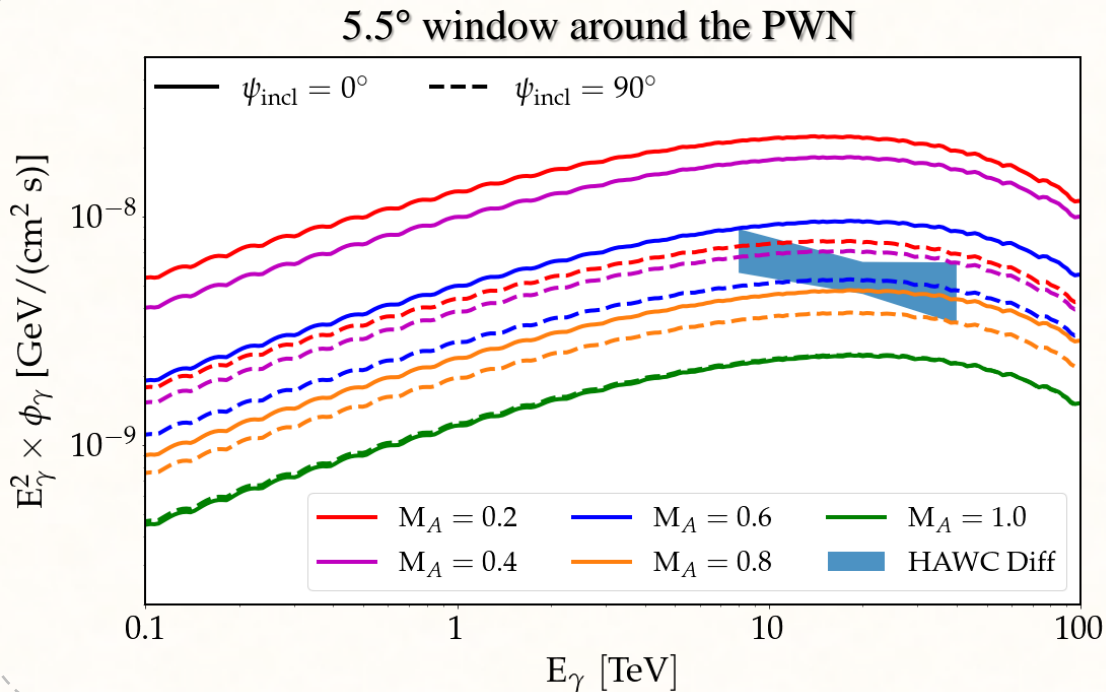
Normalized by imposing $W_e = 1.1 \times 10^{49}\ erg$.

We assume $D_\parallel = D_z = D_0 (E/E_0)^\delta$, with $E_0 = 1$ GeV, $D_0 = 3.8 \times 10^{28}$ cm²/s and $\delta = 0.33$ (Kolmogorov spectrum).

These leptons generate **$\gamma$-rays** via IC emission, which **follow the same spatial distribution as the lepton distribution** $\left(\textit{Rate of energy loss: } \frac{\partial E_e}{\partial t} \propto E_e^2\right)$

# Anisotropic diffusion

$$\frac{\partial u}{\partial t}(r, z, t, E_e) = \frac{1}{r}\frac{\partial}{\partial r}\left(rD_r\frac{\partial u}{\partial r}(r, z, t, E_e)\right) + \frac{\partial}{\partial z}\left(D_z\frac{\partial u}{\partial z}(r, z, t, E_e)\right) +$$
$$+ \mathcal{S}(r, z, t, E_e) + \frac{\partial}{\partial E_e}\left(\frac{\partial E_e}{\partial t}u(r, z, t, E_e)\right)$$

Leptons are injected with a source term following:

$$\mathcal{S}(r, z, t, E_e) = \mathcal{S}_0(1 + t/\tau_0)^{-\frac{n+1}{n-1}}\left(E_e/\text{GeV}\right)^{-\alpha}e^{-E_e/E_{\text{cut}}}\delta(r, z)$$

Normalized by imposing $W_e = 1.1 \times 10^{49}\ erg$.

We assume $D_\parallel = D_Z = D_0(E/E_0)^\delta$, with $E_0 = 1$ GeV, $D_0 = 3.8 \times 10^{28}$ cm$^2$/s and $\delta = 0.33$ (Kolmogorov spectrum).

These leptons generate **$\gamma$-rays** via IC emission, which **follow the same spatial distribution as the lepton distribution** $\left(\textit{Rate of energy loss: } \frac{\partial E_e}{\partial t} \propto E_e^2\right)$



5.5° window around the PWN

**PDTL, O. Fornieri, T. Linden (2022) ArXiv:2205.08544**

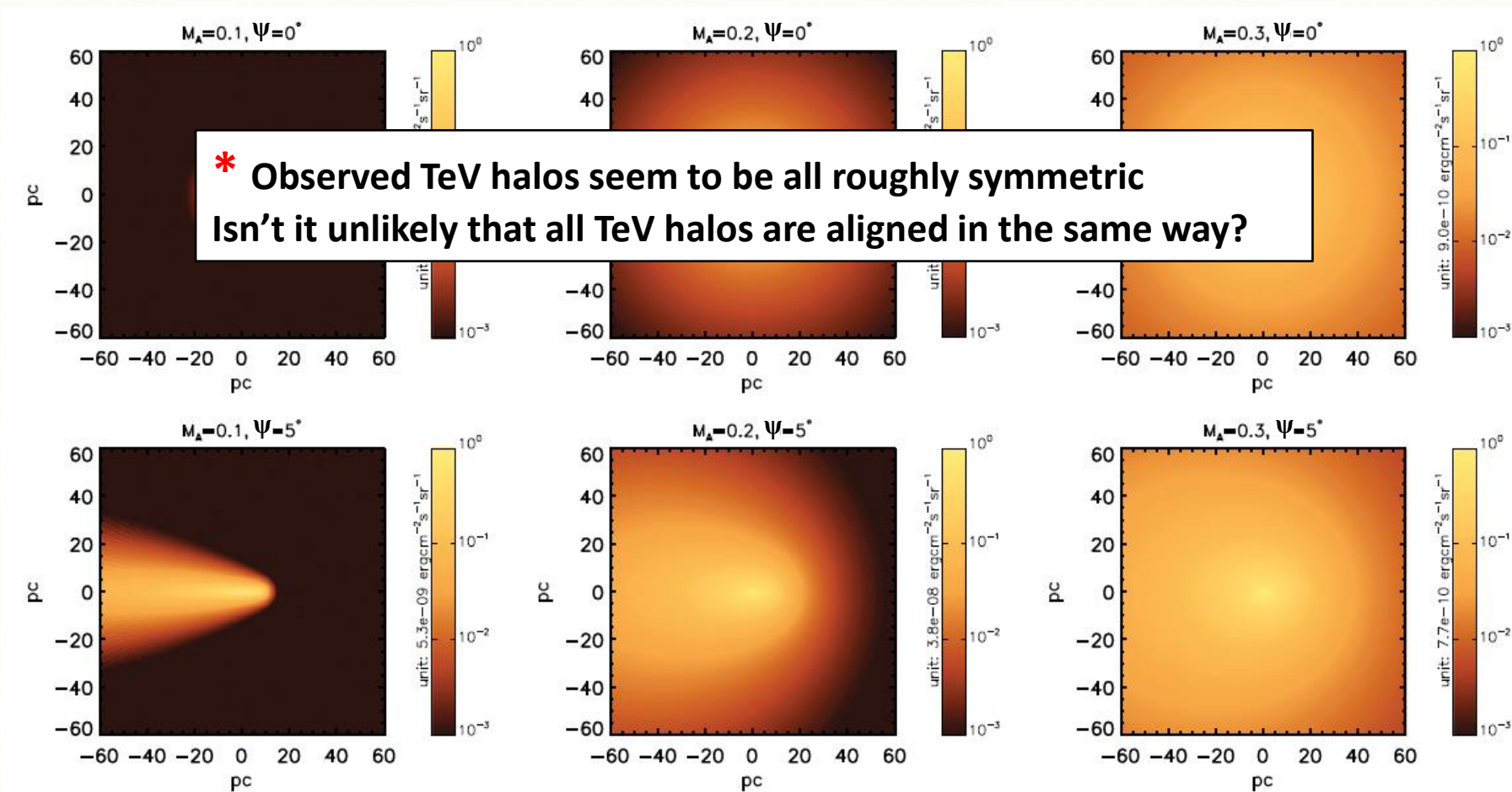# Anisotropic diffusion - Morphological consequences

**A variety of shapes and sizes is expected for different objects and inclination angles!**
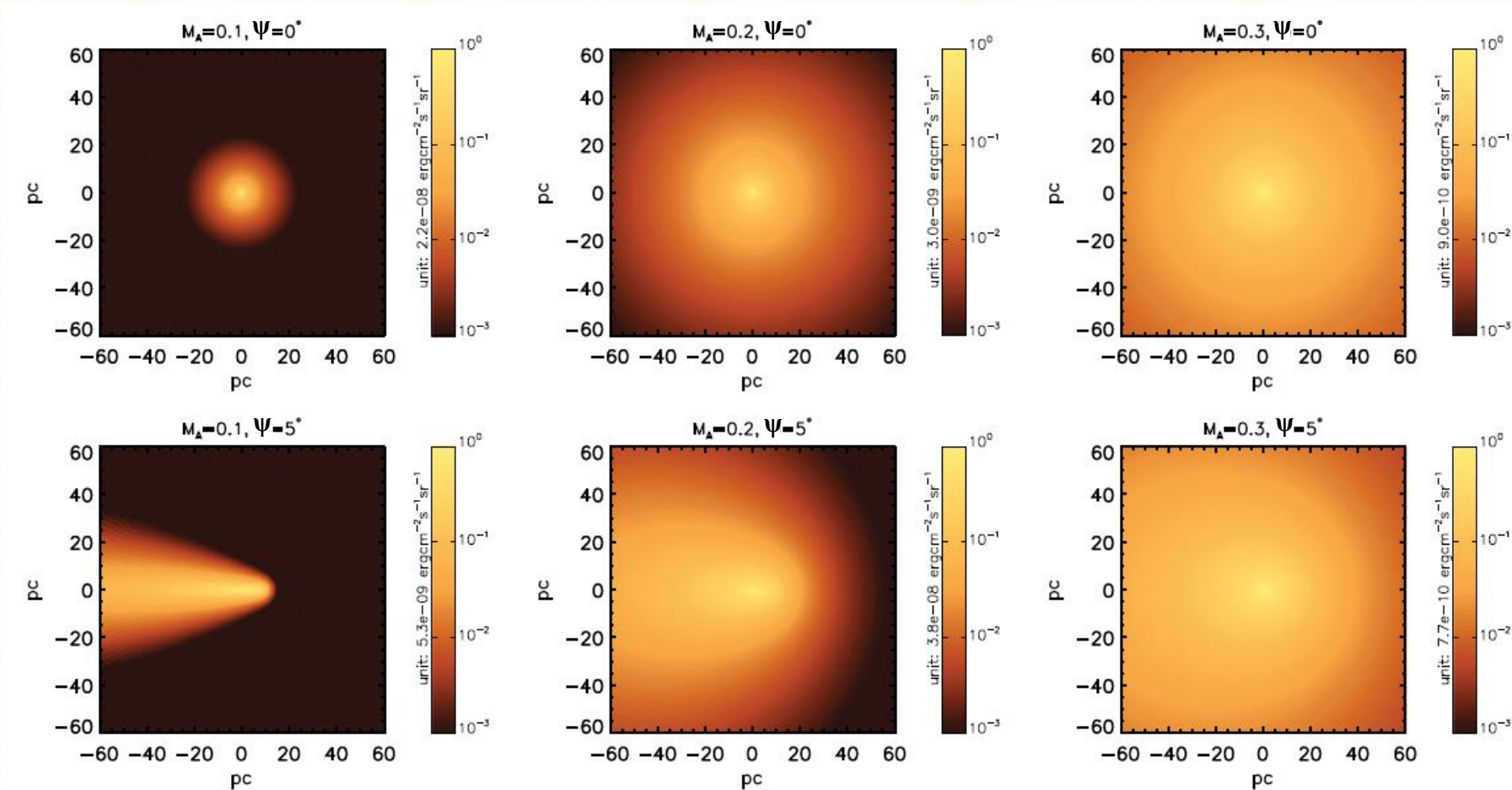


Ruo-Yu Liu et al.
PRL 123, 221103 (2019)

# Anisotropic diffusion - Morphological consequences

**A variety of shapes and sizes is expected for different objects and inclination angles!**



\* **Observed TeV halos seem to be all roughly symmetric**
**Isn't it unlikely that all TeV halos are aligned in the same way?**

Ruo-Yu Liu et al.
PRL 123, 221103 (2019)

# Parameter space allowed by TeV halo observations

We impose <u>two criteria</u> to determine the values of $\psi_{Incl}$ and $M_A$ that are **compatible with** the observations of a **few TeV halos observed** (5 out of the 11 brightest pulsars – Linden et al PRD 96, 103016, 2017) <u>based on the size of the halo along the parallel and perp. axes</u>

❖ How to estimate the "size" of a diffuse object?

Computing the percentage of particles that are contained within a given extension, so that we can quote the size of an object at a given containment (e.g. at 68% or 95% of particles contained)

❖ How to estimate if an object is symmetric?

Comparing the extension of an object in one axis with respect to the other axis

# Parameter space allowed by TeV halo observations

➢ **Size condition**: The size of the halo must be smaller than the size of the Geminga - Abeysekara et al. Science 358 6365 (2017) - to be a valid candidate. Comparison with the size of the halos at equal containment. The size depends also on the value of $D_0$!

For details: https://github.com/tospines/Analyses-and-plotting-codes/blob/main/Anisotropic_TeV_Halos/Main_numbers-TeV_Halos.ipynb
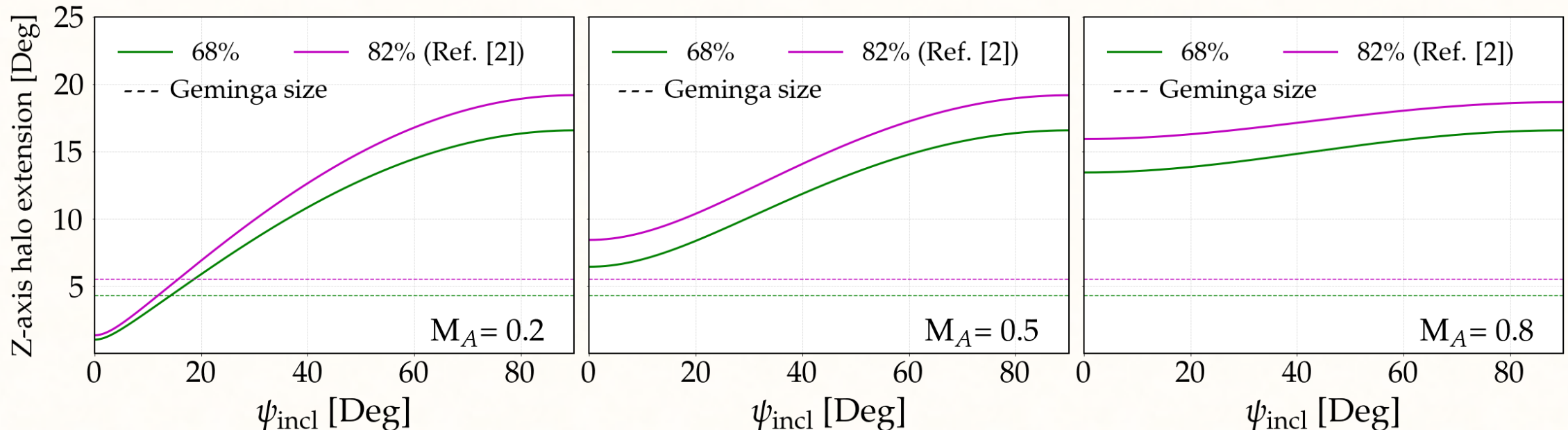
# Parameter space allowed by TeV halo observations

➢ **Symmetry condition**: Given that all TeV halos seem to be compatible with roughly symmetric shape, the extension of halo along an axis can not be much different to the extension along the other axis. We impose that **Z/R < 2**.

The larger the level of anisotropy (smaller $M_A$) the more asymmetric the halo is
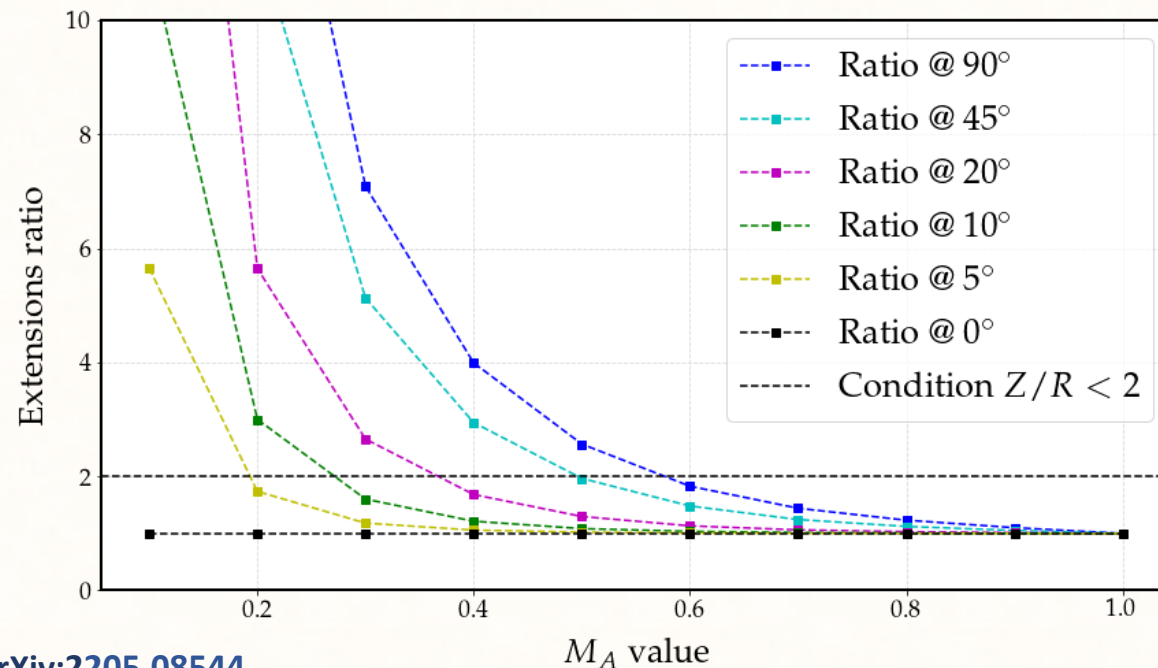


It is independent of the value of $D_0$!

# Parameter space allowed by TeV halo observations

PDTL, O. Fornieri, T. Linden (2022) ArXiv:2205.08544



$\theta_{68} < 4.3°$

$\theta_{82} < 5.5°$

$Z/R < 2$

$D_0 = 3.8 \cdot 10^{28} \text{ cm}^2/\text{s}$

(inset legend: 68%, 82%)
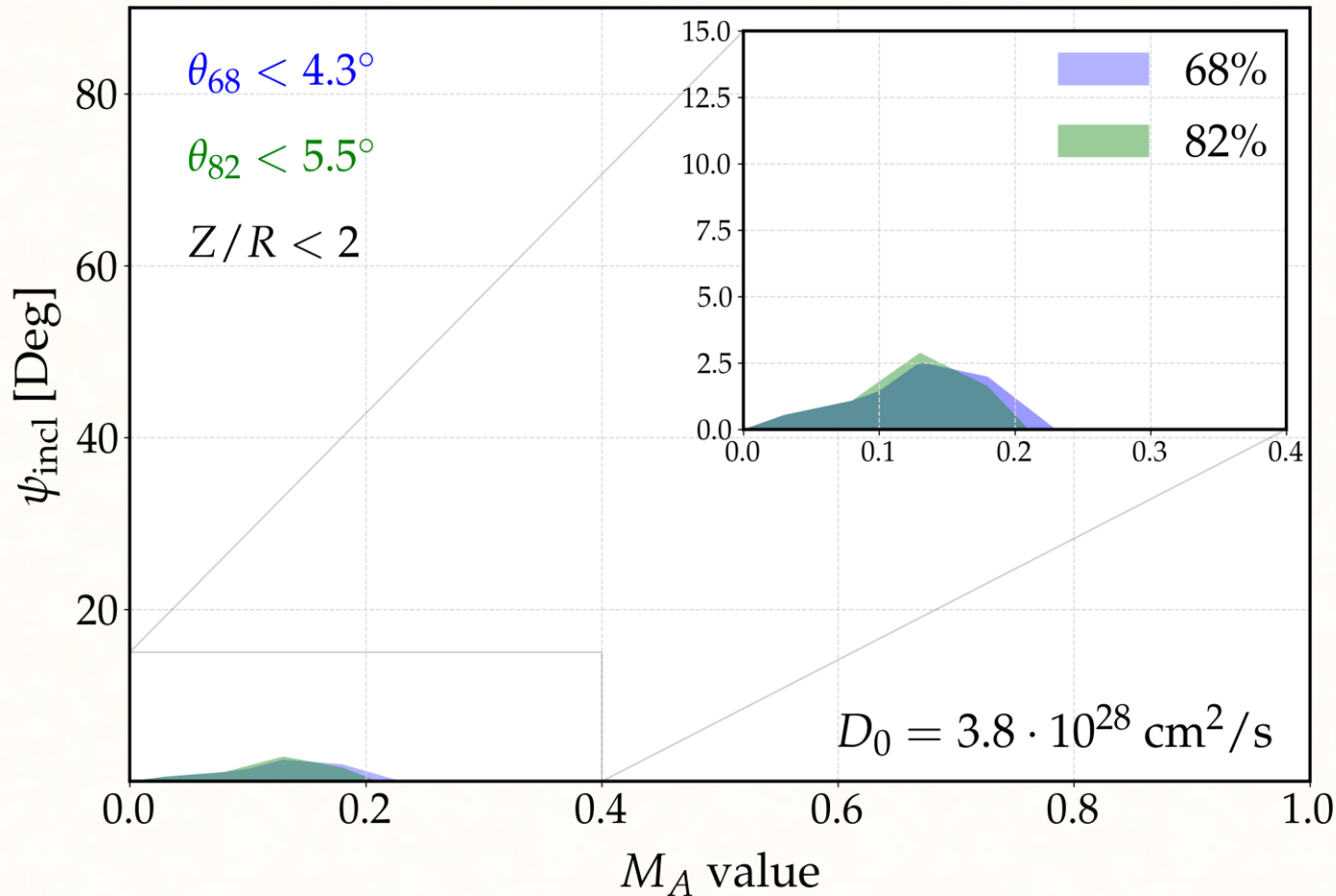
Symmetry condition: $Z/R < 2$
Size condition: $\theta_c <$ Geminga size

Only if the object is extremely well aligned with our line of sight ($\psi_{Incl} < 5°$), the halo will be compatible with the symmetry and size reported

$$P\begin{pmatrix} 5 \\ 11 \end{pmatrix} \sim 3.6 \times 10^{-10}$$

**\* It is tremendously unlikely that all TeV halos are aligned in the same way!**

17

# Why aren't there anisotropic features?

Self-generation of turbulence may explain the isotropization of the distribution of leptons.
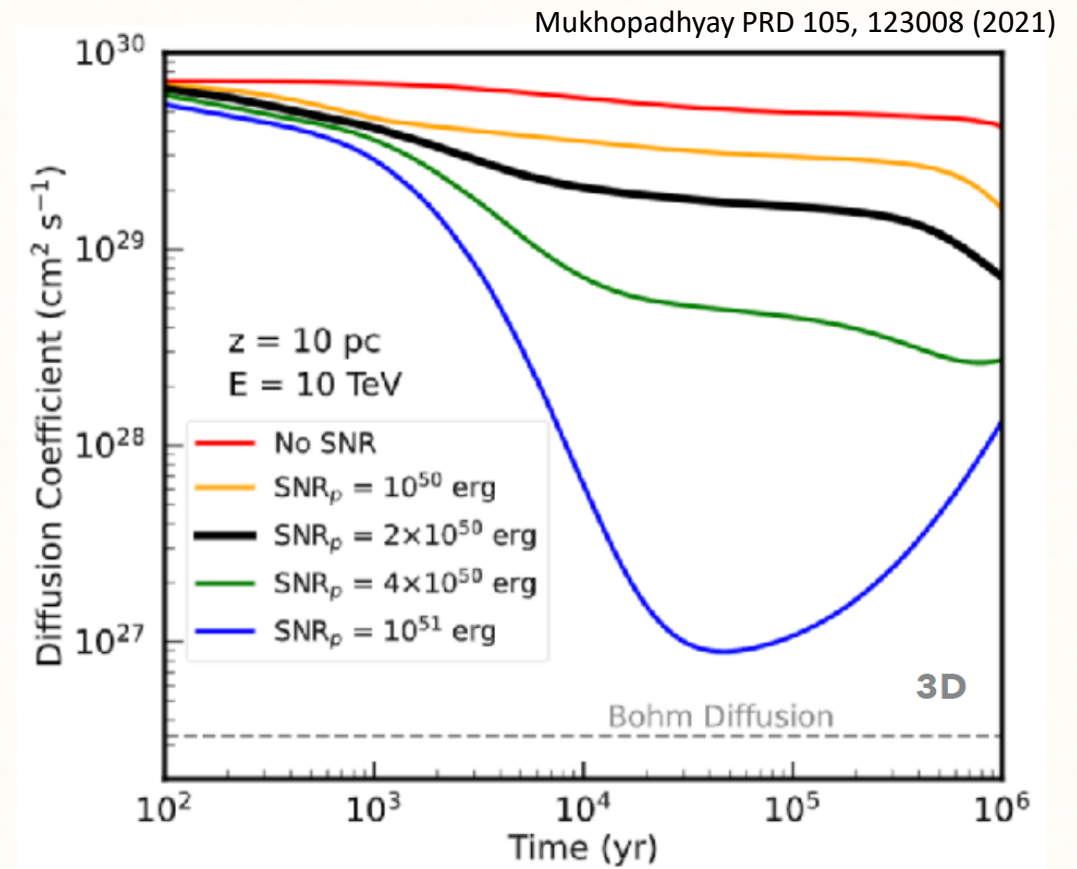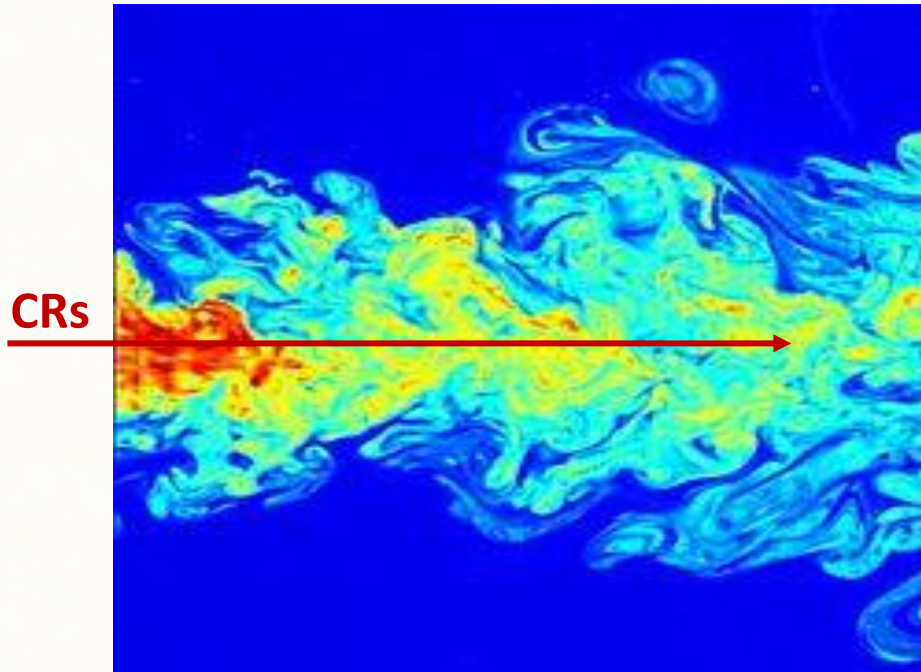
Streaming instability seems insufficient



**CRs**

# Why aren't there anisotropic features?

Self-generation of turbulence may explain the isotropization of the distribution of leptons.

Streaming instability seems insufficient



CRs



Mukhopadhyay PRD 105, 123008 (2021)
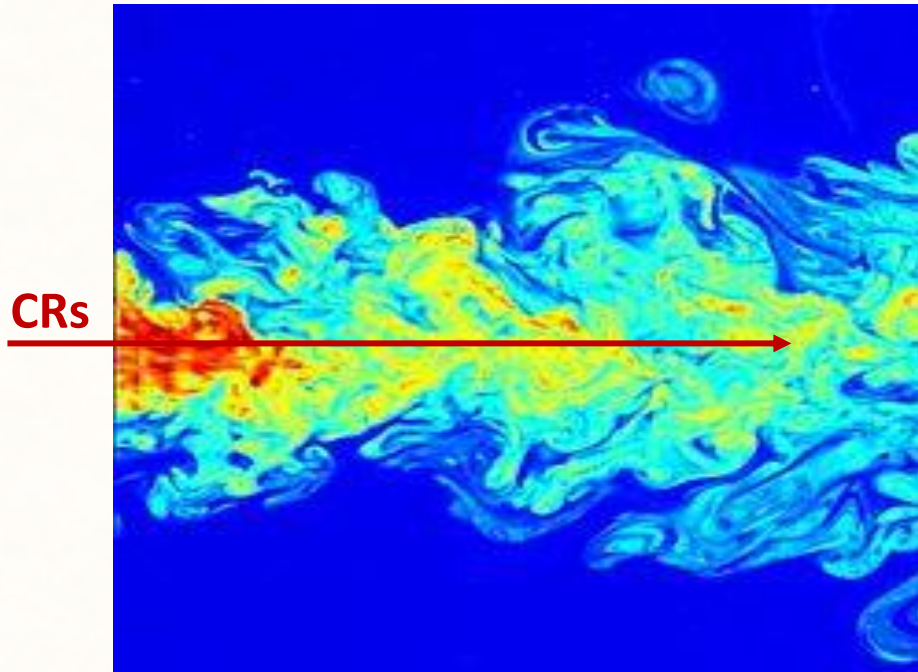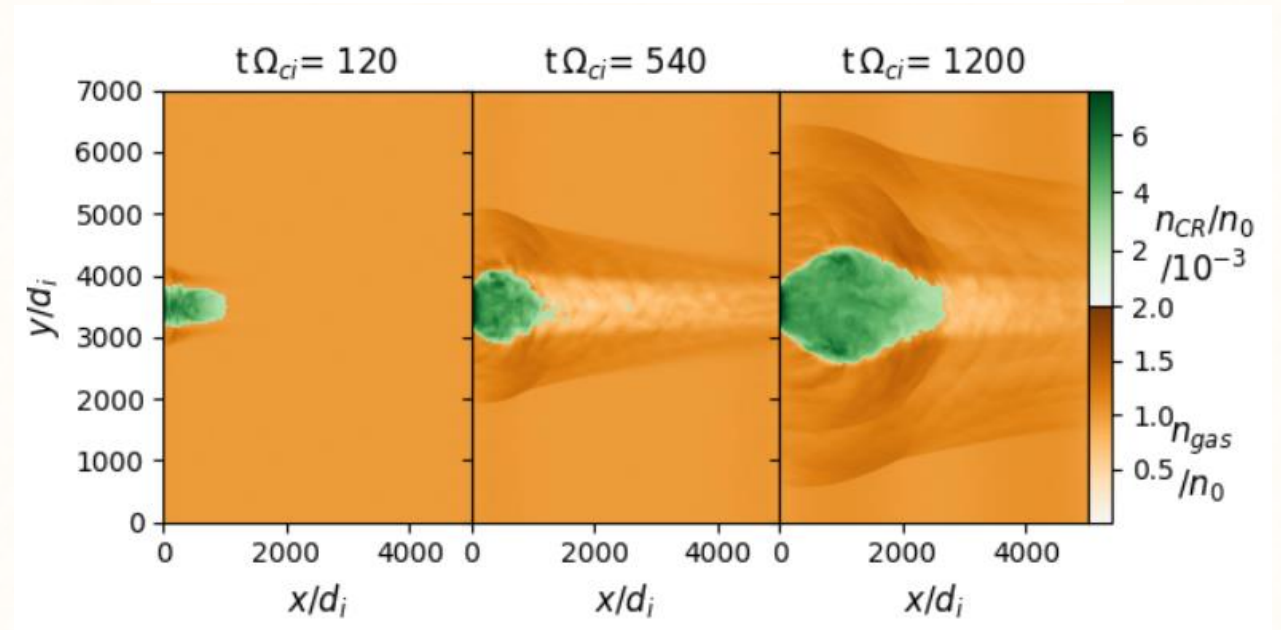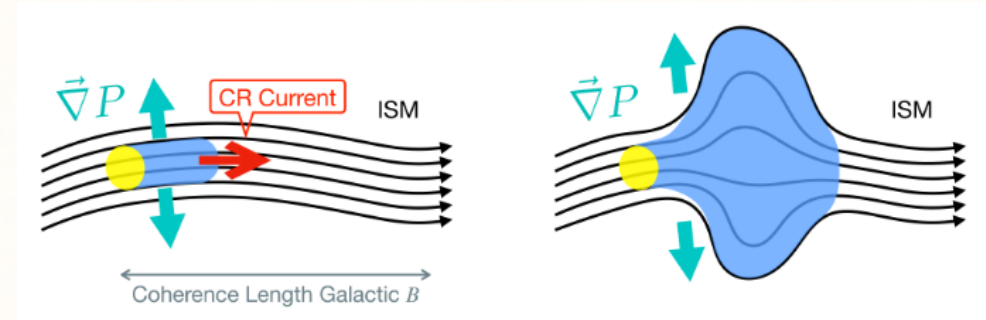
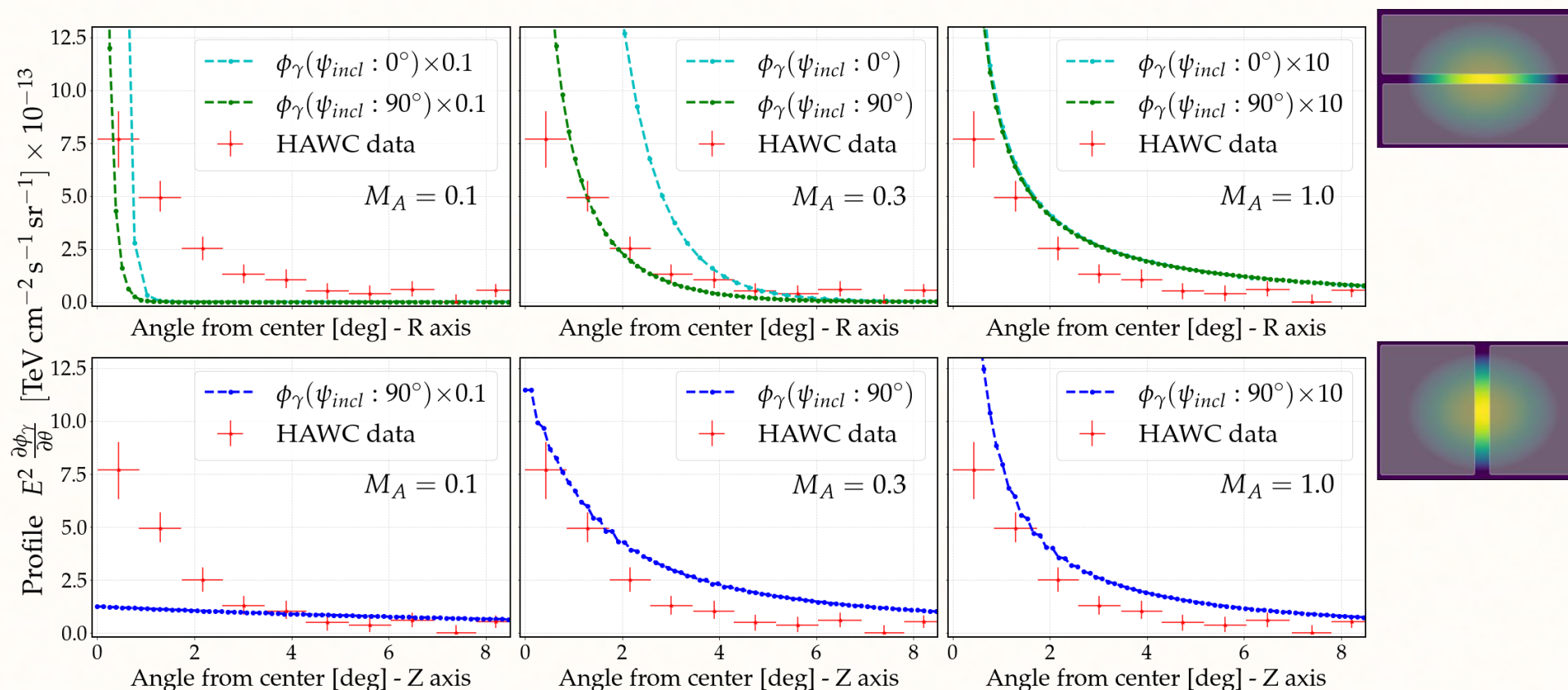# How to spot signatures anisotropic transport?

➢ Use ellipsoid/oval templates instead of gaussians to search for TeV sources
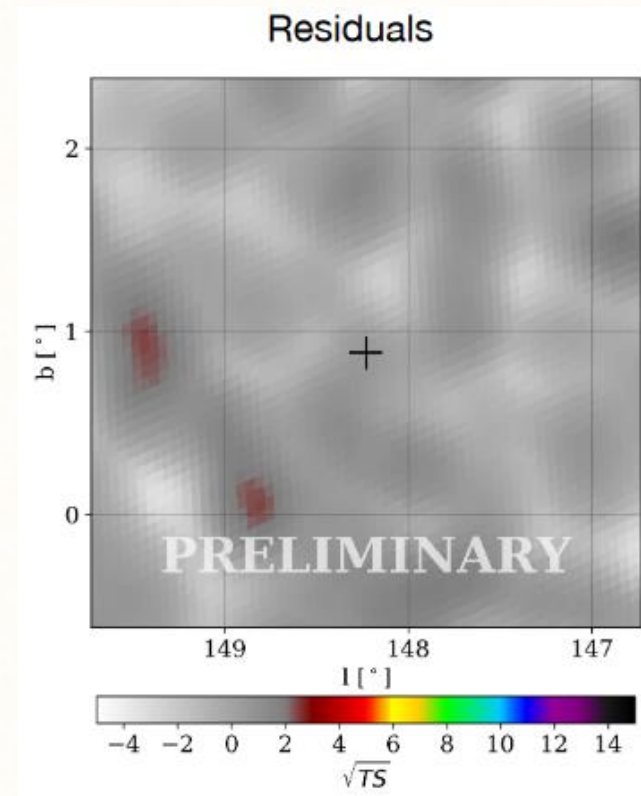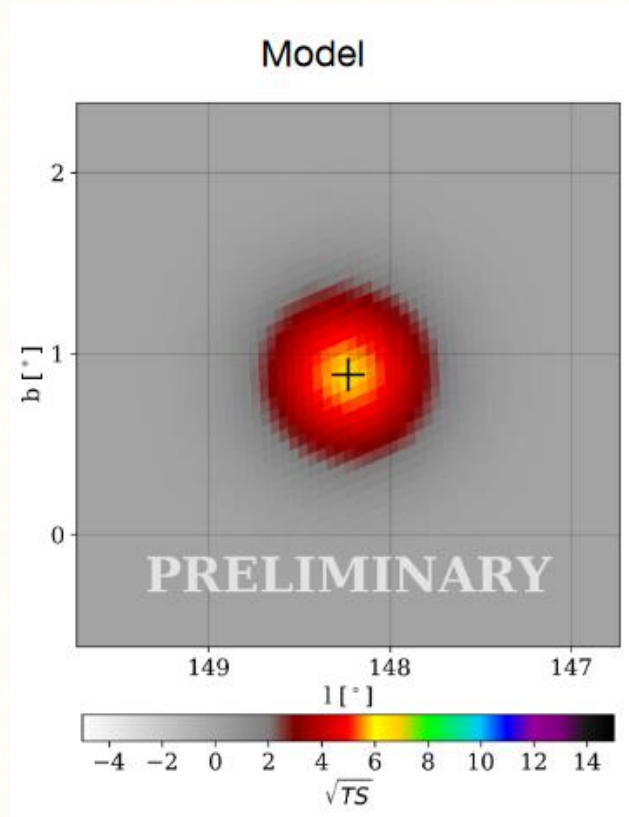


Sara Coutiño de León
Talk at $\gamma - 2022, Barcelona$

# How to spot signatures anisotropic transport?

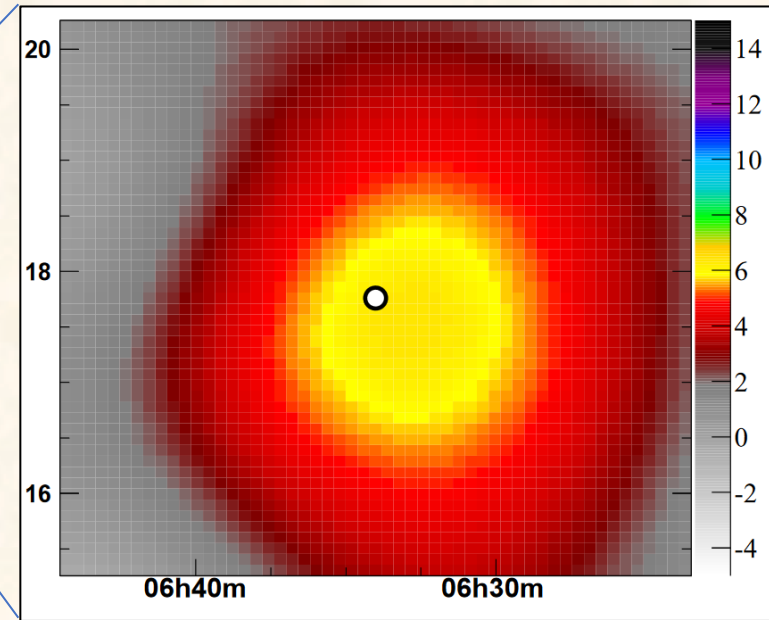➢ Surface brightness assumes symmetry! → Report the profile along different directions
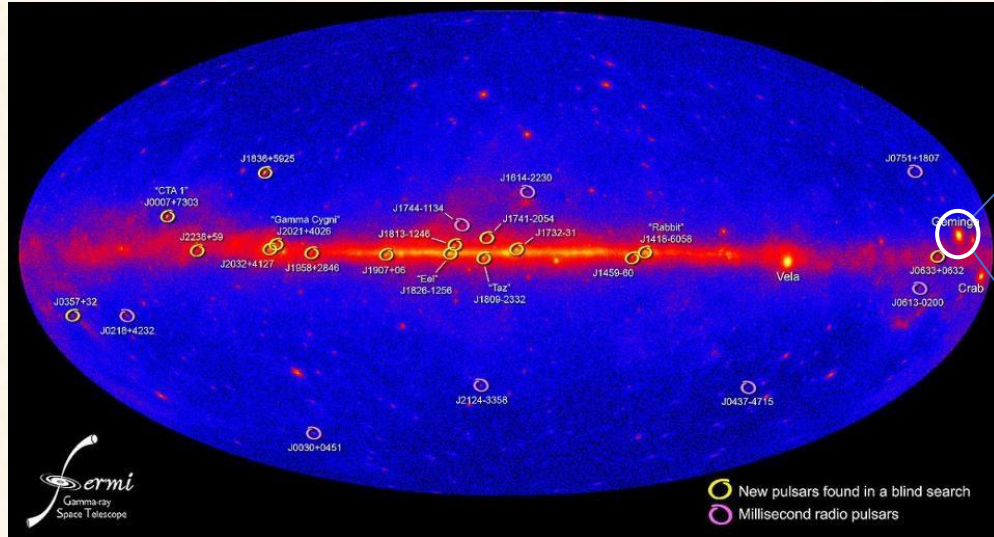
# Conclusions

o **TeV halos** are newly discovered sources that allow us to improve our understanding on the interactions of particles with plasma turbulence

o **Need of more observations** to stablish the nature and "commonness" of TeV halos. The emission from these objects can have important implications in the measurements of leptons at Earth and the diffuse gamma-ray emission

o **Anisotropic diffusion as the production mechanism** of TeV halos seems to be **tremendously unlikely**, although dedicated searches for anisotropic features are need!

o <u>Self-generation of turbulence</u> could explain why we do not observe anisotropic signatures of diffusion but the knowledge on the instabilities triggered by cosmic rays is very limited yet... **Stay tuned!**

**Pedro de la Torre Luque**    Stockholm University    pedro.delatorreluque@fysik.su.se

# BACK-UP slides

# Anisotropic diffusion cannot explain TeV halo observations

**P. De la Torre Luque (OKC, Stockholm), O. Fornieri (GSSI, Italy), T. Linden (OKC, Stockholm)**

# Why to study TeV halos?

- Injection mechanism of PWNe  (PeVatrons?)

- Environments of PWNe and SNRs as well as the mechanism of gamma-ray emission, pulsar evolution, ...

- Background diffuse gamma-ray spectrum in the Galaxy (Astrophysical plasmas, magnetic fields, ionization rates in MCs)

- Galaxy formation   See Semenov et al (2021) 2012.01427
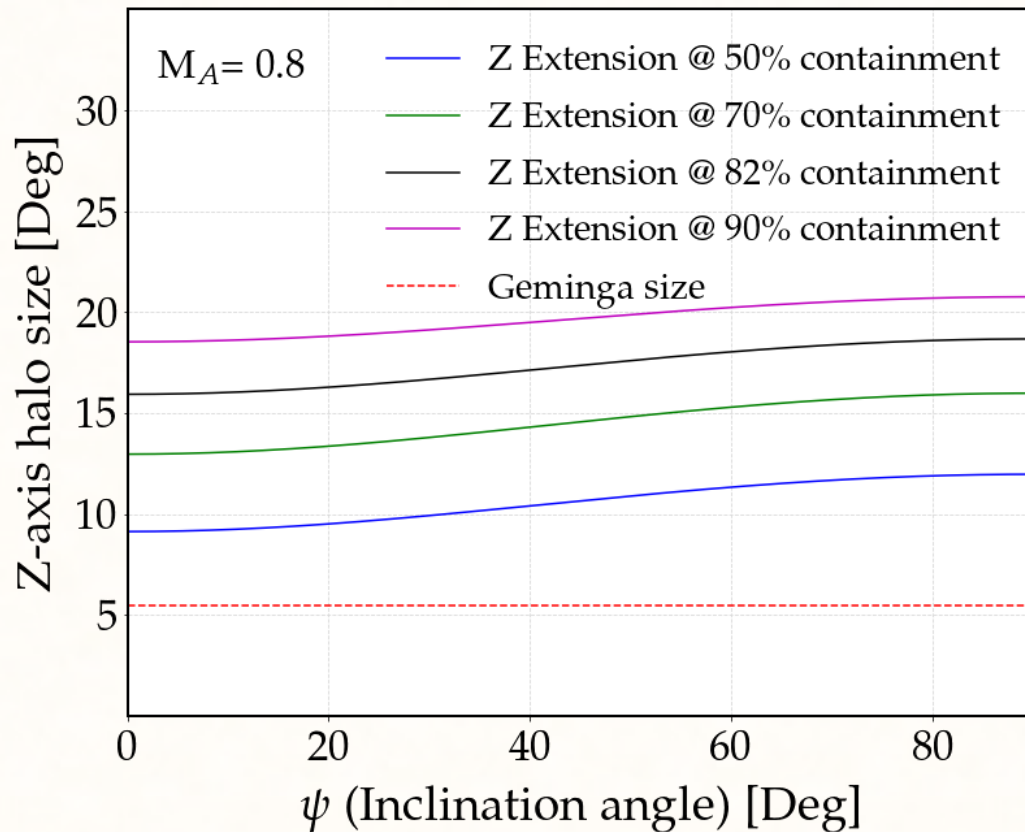
- CR lepton spectrum (DM hints?)

# A few basics

- Charged particles are accelerated at shocks! Both in SNRs and in PWN

- These sources are bright in gamma rays due to hadronic and leptonic emission processes

- Diffusion occurs because of scattering of charged particles with MHD waves
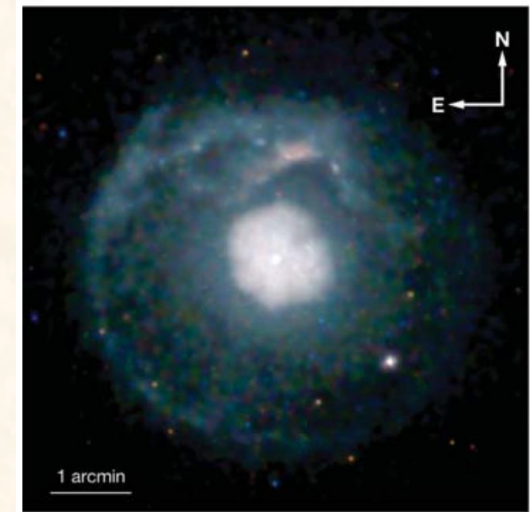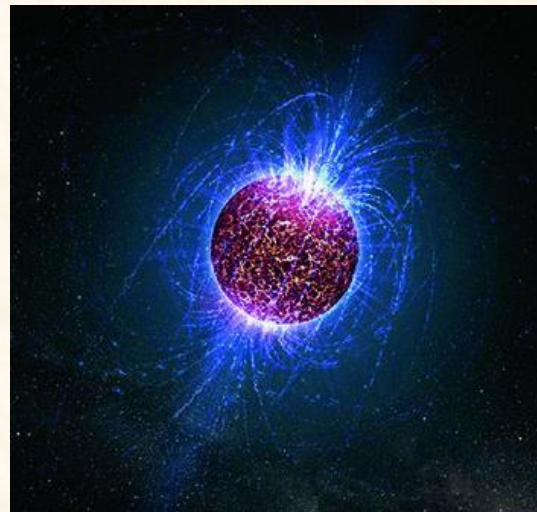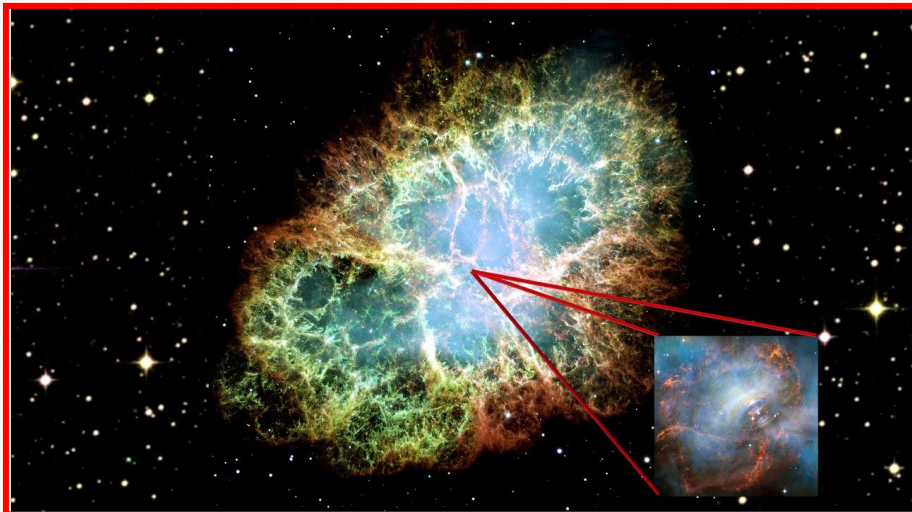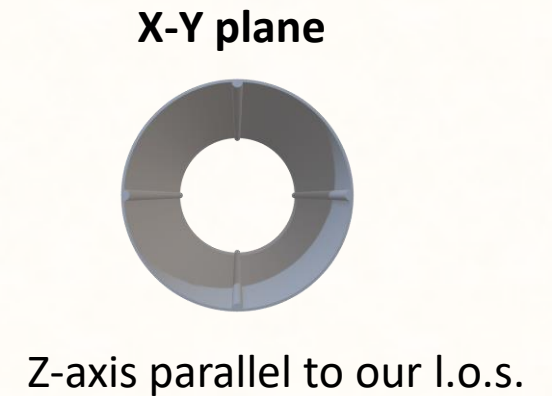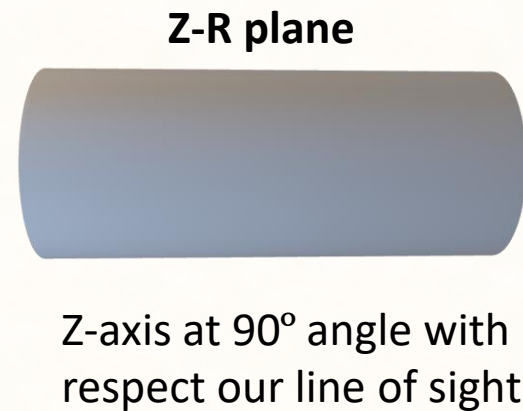
# Anisotropic diffusion

$$\frac{\partial u}{\partial t}(r,z,t,E_e) = \frac{1}{r}\frac{\partial}{\partial r}\left(rD_r\frac{\partial u}{\partial r}(r,z,t,E_e)\right) + \frac{\partial}{\partial z}\left(D_z\frac{\partial u}{\partial z}(r,z,t,E_e)\right) +$$

$$+ \mathcal{S}(r,z,t,E_e) + \frac{\partial}{\partial E_e}\left(\frac{\partial E_e}{\partial t}u(r,z,t,E_e)\right)$$



The size of the object depends on the angle at which we observe it!

**Z-R plane**                    **X-Y plane**



Z-axis at 90° angle with respect our line of sight

Z-axis parallel to our l.o.s.

**\*** **It is tremendously unlikely that all TeV halos are aligned in the same way**

# PWN around the pulsar (lepton emission)

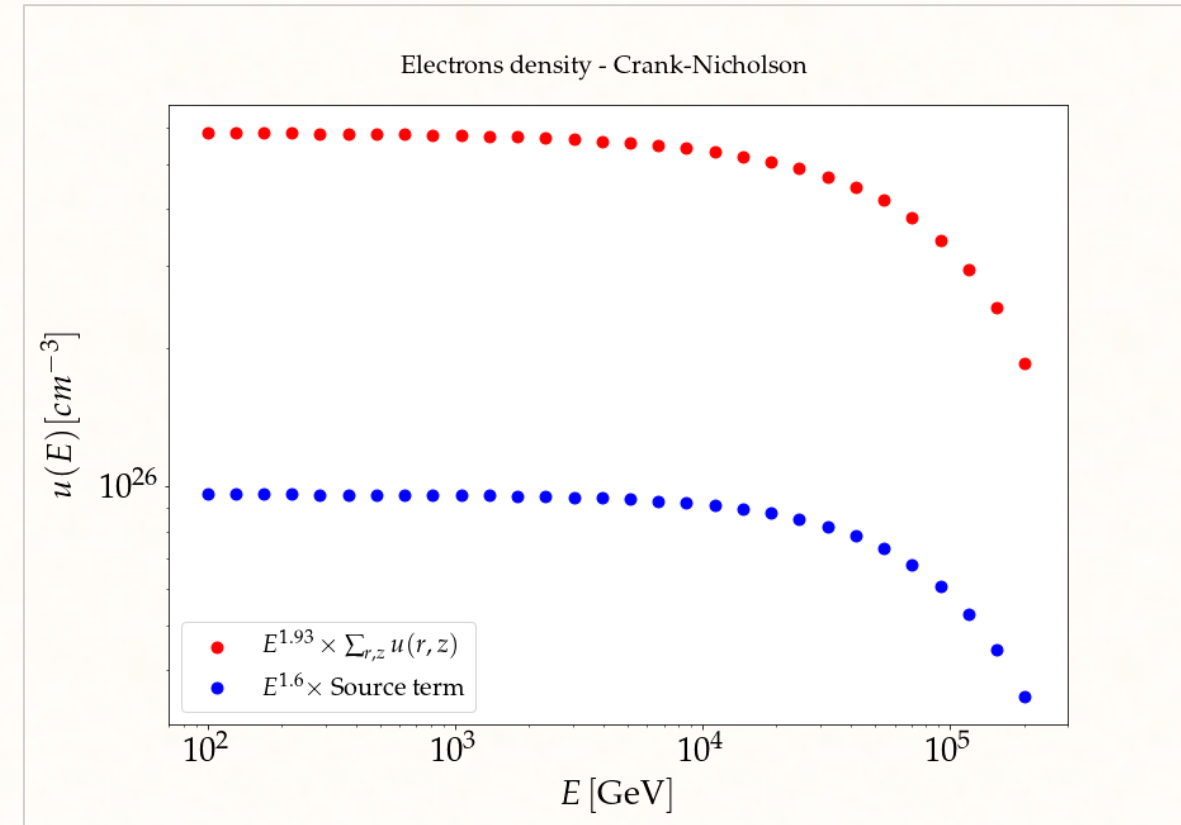$$Q(E) \sim Q_0 \, E^{-\gamma} \ \text{ with } \gamma = 1.6$$

# Diffusion coefficient

$$D \sim D_0 \frac{E^\delta}{1\text{GeV}} \text{ with } \delta = 1/3$$

$$\lambda_c \approx 0.3 \, D_{0,28} \frac{E^\delta}{1\text{GeV}} \text{ pc } \text{ with } D_{0,28} = 3.8$$
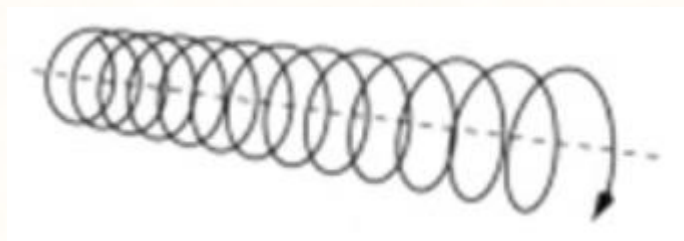
# Inhomogeneous diffusion (w.r.t. the pulsar **B**)

$$D_\perp = M_A{}^4 \, D_\parallel$$



Electrons density - Crank-Nicholson

$E^{1.93} \times \sum_{r,z} u(r,z)$
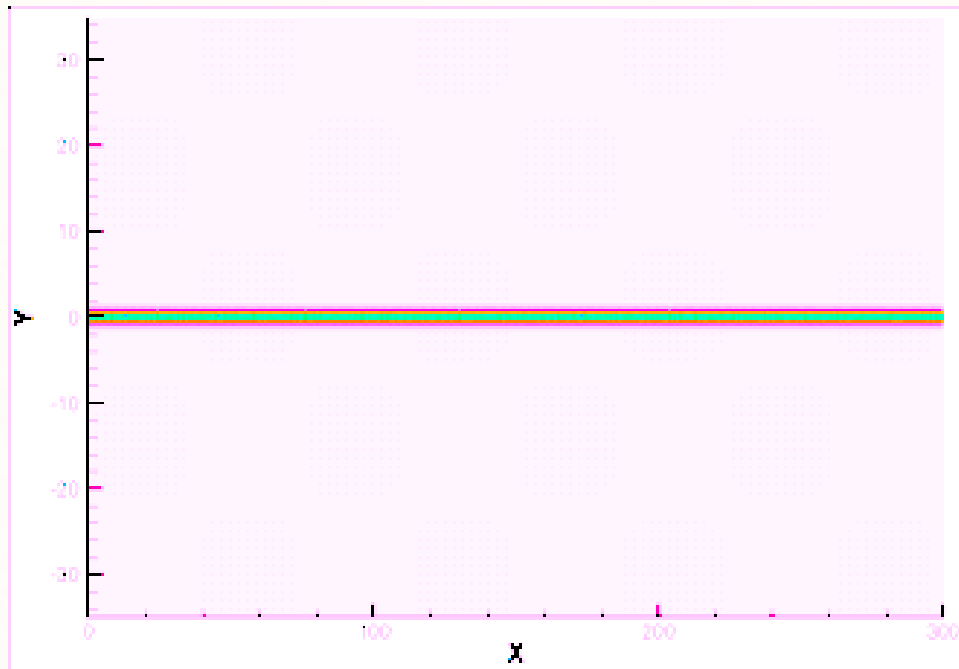
$E^{1.6} \times$ Source term

$$\frac{\partial u}{\partial t}(r, z, t, E_e) = \frac{1}{r} \frac{\partial}{\partial r} \left( r D_r \frac{\partial u}{\partial r}(r, z, t, E_e) \right) + \frac{\partial}{\partial z} \left( D_z \frac{\partial u}{\partial z}(r, z, t, E_e) \right) +$$
$$+ \mathcal{S}(r, z, t, E_e) + \frac{\partial}{\partial E_e} \left( \frac{\partial E_e}{\partial t} u(r, z, t, E_e) \right)$$

# The **Milky Way** *is a magnetised plasma medium following the*
*Magnetohydrodynamic equations*



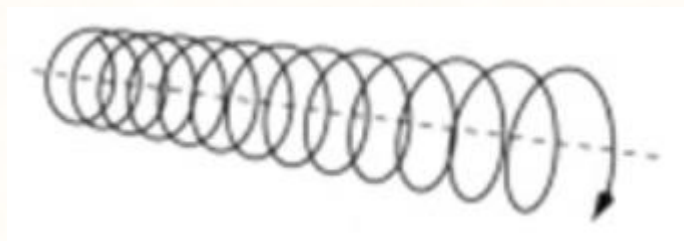$$\mathbf{B} = \mathbf{B}_0 + \delta\mathbf{B} \quad \Rightarrow \quad \langle\mathbf{B}\rangle = \mathbf{B}_0$$

$$\mathbf{E} = 0 + \delta\mathbf{E} \quad \Rightarrow \quad \langle\mathbf{E}\rangle = 0$$



**The generation of waves in the interstellar plasma makes things a lot more complex!**
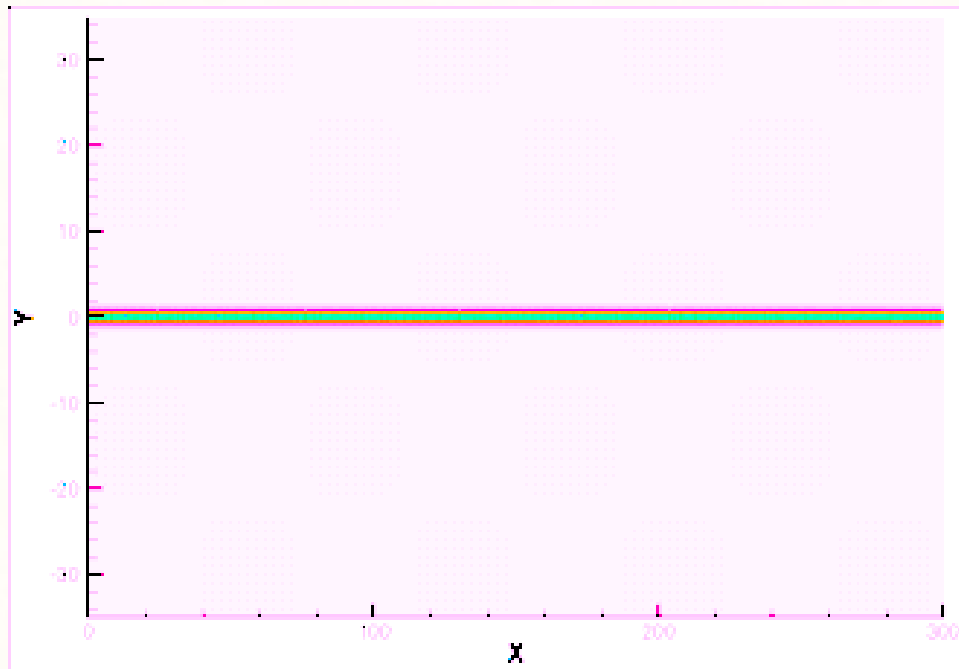
**Plasma waves are generated from <u>instabilities</u> in the chill plasma medium. This creates <u>turbulence</u> that cascade from higher to smaller scales propagating <u>waves</u> that exchange energy and momentum with cosmic rays and the plasma itself**

# The **Milky Way** *is a magnetised plasma medium following the Magnetohydrodynamic equations*
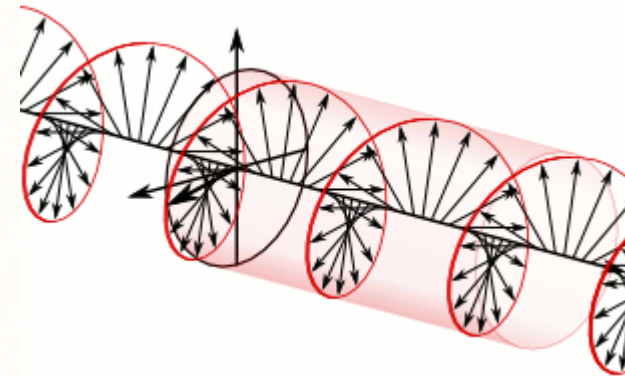


$$B = B_0 + \delta B \quad \Rightarrow \quad <B> = B_0$$

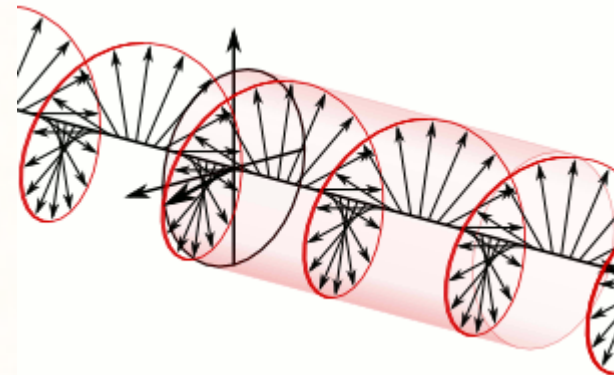$$E = 0 + \delta E \quad \Rightarrow \quad <E> = 0$$



Alfven waves are circularly polarized whose resonant interaction governs the CR scattering

# The **Milky Way** *is a magnetised plasma medium following the*

*Magnetohydrodynamic equations*
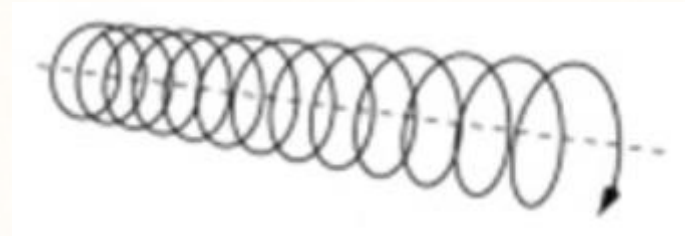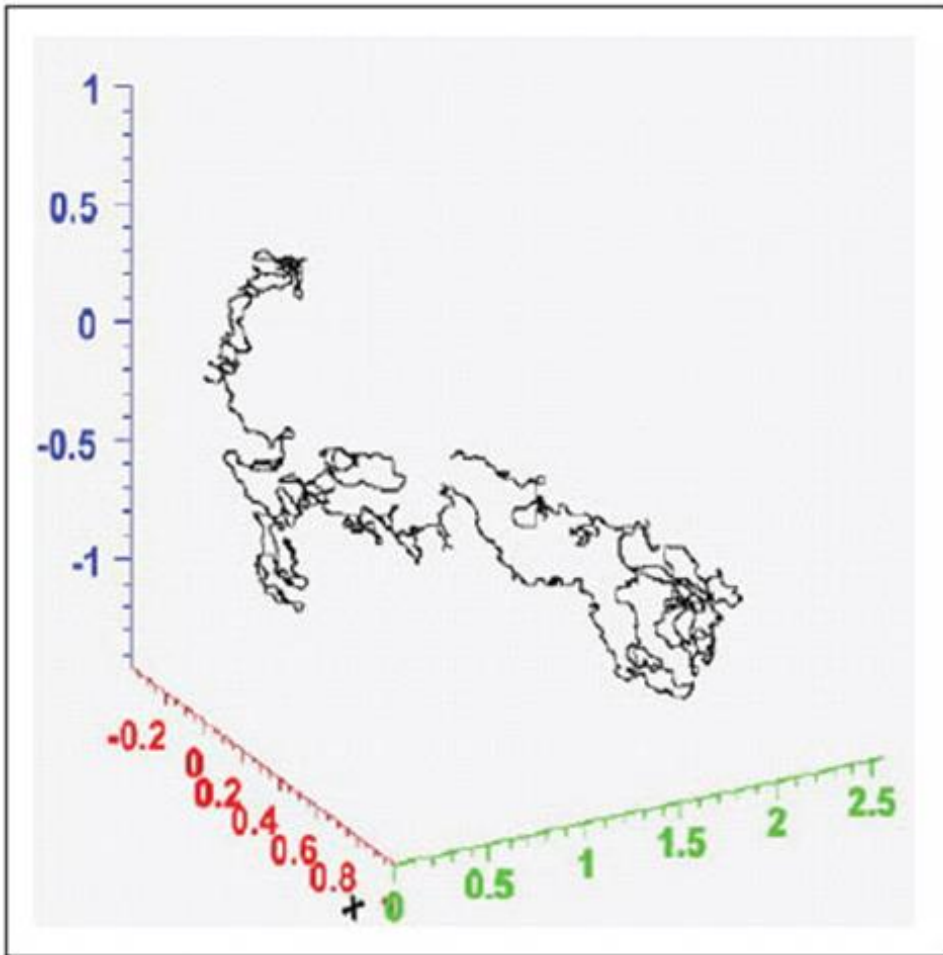




Alfven waves are circularly polarized whose resonant interaction governs the CR scattering

# TeV halo candidate list from the Third HAWC Catalog (3HWC, Albert et al. 2020) for a 1523-day data set (November 2014, June 2019)

| HAWC | $l$ (°) | $b$ (°) | Pulsar | Age (kyr) | $\dot{E}$ (erg s$^{-1}$) | Distance (kpc) | Separation (°) | TeVCat |
|------|---------|---------|--------|-----------|--------------------------|----------------|----------------|--------|
| 3HWC J0540+228 | 184.58 | −4.13 | B0540+23 | 253.0 | 4.09e+34 | 1.56 | 0.83 | HAWC J0543+233 |
| 3HWC J0543+231 | 184.67 | −3.52 | B0540+23 | 253.0 | 4.09e+34 | 1.56 | 0.36 | HAWC J0543+233 |
| 3HWC J0631+169 | 195.63 | 3.45 | J0633+1746 | 342.0 | 3.25e+34 | 0.19 | 0.95 | Geminga |
| 3HWC J0634+180 | 195.00 | 4.62 | J0633+1746 | 342.0 | 3.25e+34 | 0.19 | 0.38 | Geminga Pulsar |
| 3HWC J0659+147 | 200.60 | 8.40 | B0656+14 | 111.0 | 3.8e+34 | 0.29 | 0.51 | 2HWC J0700+143 |
| 3HWC J0702+147 | 200.91 | 9.01 | B0656+14 | 111.0 | 3.8e+34 | 0.29 | 0.77 | 2HWC J0700+143 |
| 3HWC J1739+099 | 33.89 | 20.34 | J1740+1000 | 114.0 | 2.32e+35 | 1.23 | 0.13 | ... |
| 3HWC J1831-095 | 22.13 | 0.02 | J1831−0952 | 128.0 | 1.08e+36 | 3.68 | 0.27 | HESS J1831-098 |
| 3HWC J1912+103 | 44.50 | 0.15 | J1913+1011 | 169.0 | 2.87e+36 | 4.61 | 0.31 | HESS J1912+101 |
| 3HWC J1923+169 | 51.58 | 0.89 | J1925+1720 | 115.0 | 9.54e+35 | 5.06 | 0.67 | ... |
| 3HWC J1928+178 | 52.93 | 0.20 | J1925+1720 | 115.0 | 9.54e+35 | 5.06 | 0.85 | 2HWC J1928+177 |
| 3HWC J2031+415 | 80.21 | 1.14 | J2032+4127 | 201.0 | 1.52e+35 | 1.33 | 0.11 | TeV J2032+4130 |

**Note.** The age of the pulsar in kyr and the spin-down luminosity, $\dot{E}$, in erg s$^{-1}$ are also given. The Separation column indicates the angular distance between the HAWC source and the ATNF pulsar (Manchester et al. 2005). The TeVCat column lists the previously detected TeV counterpart of each source.

# Abeysekara et al 2017
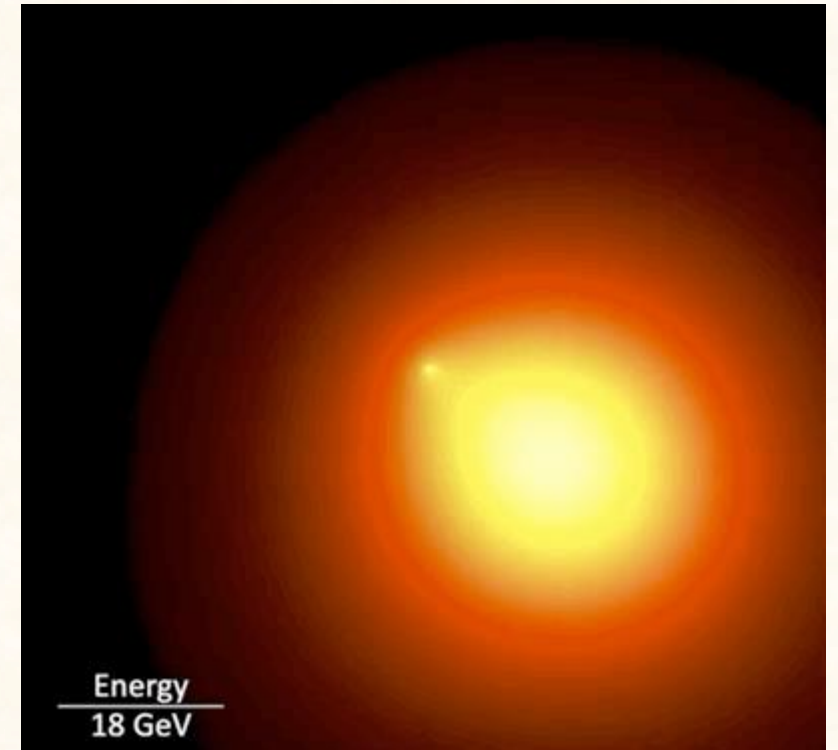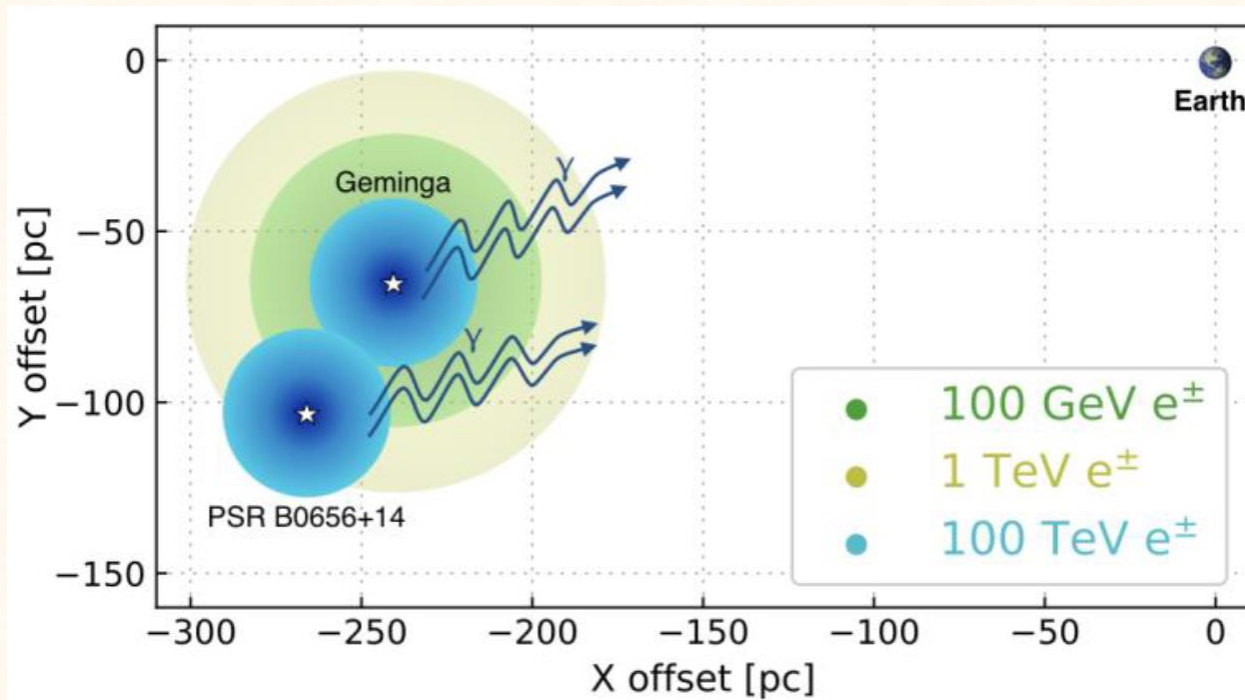
Dependence of the flux with the size of the object

$$\frac{dN}{d\Omega} = \frac{1.22}{\pi^{3/2}\theta_{\mathrm{d}}(E)(\theta + 0.06\theta_{\mathrm{d}}(E))} \times \exp\left[-\frac{\theta^2}{\theta_{\mathrm{d}}(E)^2}\right]$$

$$\theta_{\mathrm{d}} = \frac{180}{\pi}\frac{R_{\mathrm{diff}}}{d_{\mathrm{src}}}$$

$$R_{\mathrm{diff}} = 2\sqrt{D(E_{\mathrm{e}})t_{\mathrm{e}}}$$

$t_{\mathrm{e}}$ is the cooling time.

At E ≤ ~100 GeV the object seems asymmetric because of its movement and the fact that at these energies $\pi^0$ decay is the main source of gamma rays





NASA's Goddard Space Flight Center/M. Di Mauro

# Ballistic propagation preceding diffusive propagation

S. Recchia+ (2021)